

Light-folded projection three-dimensional display

Jaehyuk Jang,¹ Jongwoo Hong,¹ Hwi Kim,² and Joonku Hahn^{1,*}

¹School of Electronics Engineering, Kyungpook National University, 1370 Sankyuk-dong, Buk-gu, Daegu 702-701, South Korea

²Department of Electronics and Information Engineering, College of Science and Technology, Korea University, Sejong Campus, Sejong-ro 2511, Sejong 339-700, South Korea

*Corresponding author: jhahn@knu.ac.kr

Received 3 December 2012; revised 27 February 2013; accepted 27 February 2013;
posted 28 February 2013 (Doc. ID 181005); published 29 March 2013

A light-folded projection three-dimensional (3D) display system with a single projection lens and a rectangular light tunnel which is composed of four folding mirrors on its inside walls is proposed. It is theoretically shown through the Wigner distribution function analysis that the proposed system can generate the same light field effectively as that of the conventional projection-type multiview 3D display system with plural projection lenses. Multiview 3D imaging of the proposed system configuration is experimentally demonstrated. © 2013 Optical Society of America
OCIS codes: 100.6890, 110.2990.

1. Introduction

Conventional three-dimensional (3D) displays can be classified with respect to the type of imaging optics used in the systems [1,2]. Projection-type 3D display is referred to the display with plural projection lenses that are used to project directional images on a fixed common imaging window [3–6]. Holographic 3D or volumetric 3D displays produce natural 3D light field having 3D shape structure in free space [7,8], but the projection-type 3D display generates several directional projection images focused on a common specified imaging window.

The projection-type 3D display provides distinct number of views according to observing positions and this disparity among views results from the difference of the positions of projection lenses. In the projection-type 3D display, there exists a trade-off between the number of views and the resolution of each view [9]. This is natural since the number of pixels in a directional view is finite and it has resemblance as the invariant property of space-bandwidth product in holographic displays [10,11]. Total amount of information is determined by the summation of number of pixels of directional images. Thus, it is

impossible to increase the number of views without the cost of the resolution of each view.

Theoretically, the relation between this trade-off and the space-bandwidth product can be understood with the Wigner distribution function (WDF) [12–14]. The WDF represents that the area in two-dimensional phase space is conserved through the entire optical pathway of the optical imaging system, meaning that if the spatial frequency bandwidth increases, the space bandwidth decreases consequently.

From several reasons, folding optics using mirrors has been applied for projection-type 3D displays. Balogh and co-workers presented the hologram-like display with two folding mirrors on both ends of one-dimensional array of projection lenses [15,16]. By reflection from side mirrors, the observer feels that there are fictitious projection lenses outside the boundaries defined by the side mirrors and sees 3D images with enlarged viewing angle. This mirroring effect was applied to increase the uniformity in the bandwidth of the angular spectrum [17].

In this paper, we propose a projection-type 3D display with a single projection lens. This has a light tunnel structure folding the propagating light field inside it. The light tunnel consists of four mirrors positioned parallel and its shape is a rectangular column. Figure 1 shows a schematic of the system. The elemental images are transferred by the projection

1559-128X/13/102162-07\$15.00/0
© 2013 Optical Society of America

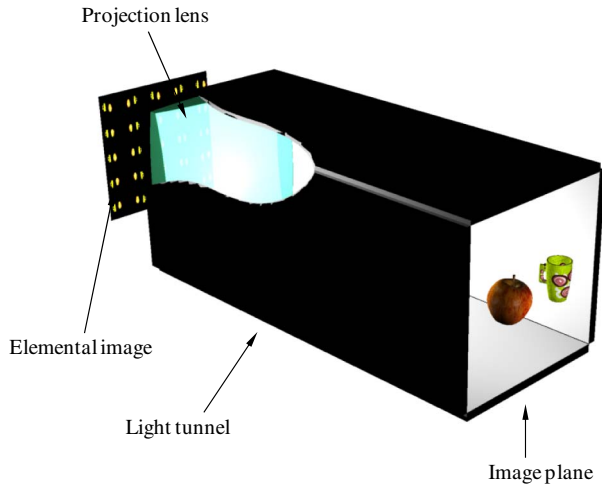


Fig. 1. (Color online) Schematics of 3D light-folded display with one projection lens and the light tunnel composed of light-folded mirrors.

lens and folded by reflection on the mirrors. Since the number of reflection is different according to the position of the elemental image, it results in the change of the direction of the view and every view is overlapped at the same rectangular image plane on the exit of the light tunnel.

This paper is organized as follows. In Section 2, folding of the view is interpreted in the phase space in terms of WDF. In Section 3, we explain the method to generate elemental images with consideration of the folding effect according to the positions of elemental images. In Section 4, experimental results are presented and the negative effect induced from possible misalignments of mirrors is discussed. In Section 5, conclusion and perspective are given.

2. Folding Effect Interpreted by Wigner Distribution Function

The WDF is useful to design and analyze the wave optic system since it represents wave optic propagation with ray-based concept using the four-dimensional WDF of both space and local spatial frequency. With

WDF analysis, the system is interpreted by tracing ray-bundle. One important property of the WDF is that it represents geometrically how the information of the light field distribution is configured. Therefore, especially for a given 3D display, the number of views and the resolution of each view are clearly understood with the WDF analysis.

Figure 2 shows the coordinates defined for a projection lens system. Along an optical axis, three planes exist sequentially. The first is an elemental image plane where a two-dimensional array of images is positioned and the second is a projection lens plane where the projection lens is simply assumed as a thin lens and this plane is also an aperture stop plane. The last is an image plane where elemental images are projected and overlapped. The distances between first two planes and between last two planes are d_1 and d_2 , respectively. The propagation of rays starting from the elemental image plane to image plane is represented with four parameters; two space coordinates and two directional cosines. The WDF with these four parameters is calculated to interpret the system.

Without loss of generality, the phase space (x, f_x) can be used for analysis because of cylindrical symmetry of the optical system. Figure 3 shows propagation of light field from the elemental image plane to the image plane through the projection lens. In this system, the WDFs at the elemental image plane, the projection lens plane, and the image plane are drawn, respectively. Here, a green dot in Fig. 3(a) is a point on the elemental image and the bundle of the rays appears as the green line in Figs. 3(b)–3(d). We are concerned with the case that the dimension of a projected image is equal to that of the aperture stop of the projection lens. The condition satisfying this case is calculated by using ray-transfer matrix technique.

In advance to analyze the fold effect, it is necessary to calculate the maximum width of the elemental image which is projected without folding. This value is used to define the view at the elemental image plane. In Fig. 3(b), the width of the elemental image is denoted as w and the half-width of the aperture

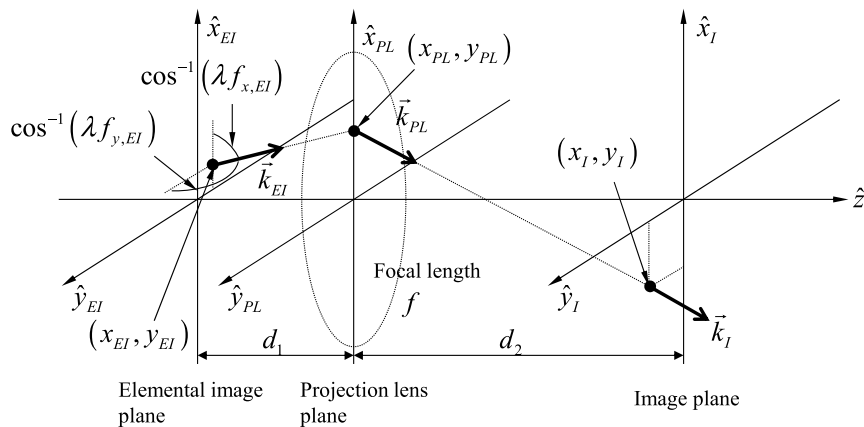


Fig. 2. Coordinates of a projection lens system. Here, the elemental image plane is projected on the image plane by a projection lens with focal length f . A ray in the elemental image plane is defined two space coordinates and two directional cosines. Its directional cosine is a product of the wavelength λ and the spatial frequency f_{EI} .

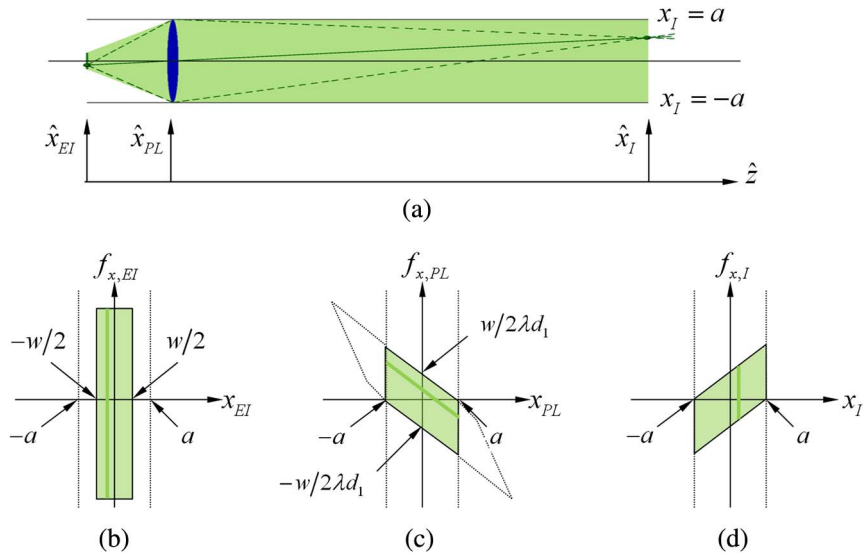


Fig. 3. (Color online) (a) Propagation of light field through the projection lens and WDFs at (b) elemental image plane, (c) projection lens plane, and (d) image plane when the dimension of a projected image is equal to that of the aperture stop of the projection lens. A green dot in Fig. 3(a) is a point on the elemental image and the bundle of the rays appears as the green line in Figs. (b)–(d).

stop is denoted as a . The aperture stop of the projection lens is determined equal to the width of the light tunnel. The position and the spatial frequency of the ray at the projection lens plane are determined, respectively, by

$$x_{PL} = x_{EI} + \lambda d_1 f_{x,EI}, \quad (1a)$$

$$f_{x,PL} = (-1/\lambda f)x_{EI} + (1 - d_1/f)f_{x,EI}. \quad (1b)$$

The WDF at the projection lens plane is shown in Fig. 3(c). By the aperture size, the WDF is cropped within $x_{PL} = -a$ and $x_{PL} = a$. As light field propagates from the projection lens plane to the image plane, the WDF becomes sheared dependent on the value of the spatial frequency. So, in order to make the WDF remain within the light tunnel, the spatial frequency at the position, $x_{PL} = a$ needs to be zero. Then the WDF at the image plane is expected, as shown in Fig. 3(d). Therefore, from Eqs. (1a) and (1b), the focal length of the projection lens is determined as

$$f = \frac{ad_1}{a + w/2}. \quad (2)$$

The width of the elemental image is obtained by

$$w = 2a \times d_1/d_2. \quad (3)$$

Next, let us think about the case that the array with 5×5 elemental images is projected. If there is no light tunnel, the light field in the system will not be folded by the mirrors at the image plane, as shown in Fig. 4(a). The WDFs at the projection lens plane and the image plane are drawn, respectively, in Figs. 4(b) and 4(c). The colors in the WDF represent

different elemental images. Every part in the WDF from individual elemental images remains within the aperture of the projection lens at the projection lens plane. Then this is sheared according to the propagation. At the image plane the partial width of the WDF from each elemental image is also equal to the aperture of the projection lens.

Figure 5 shows the light field through the system and the WDFs at several planes when the light tunnel is inserted. To show change of the WDF in details, the WDFs at the positions of $0.25d_2$ and $0.75d_2$ are, respectively, drawn in Figs. 5(b) and 5(c). When the light field is folded, the position and the sign of the spatial frequency change by the symmetry posed by the mirror surface. At the image plane, the WDF turns out to have the structure shown in Fig. 5(d) depicting that every partial WDF from individual elemental image is stacked vertically. The light field folded by the light tunnel and the unfolded light field shown in Fig. 4(a) have the relation determined by

$$x_I = \text{TriangleWave}\{x_{Unfolded}/2a\}, \quad (4a)$$

$$f_{x,I} = \text{SquareWave}\{x_{Unfolded}/2a\}f_{x,Unfolded}, \quad (4b)$$

where $\text{TriangleWave}(\cdot)$ and $\text{SquareWave}(\cdot)$ are defined, respectively, by

$$\text{TriangleWave}(x) = \frac{2}{\pi} \sin^{-1}[\sin(\pi x)], \quad (4c)$$

$$\text{SquareWave}(x) = \frac{2j}{\pi} \{ \tanh^{-1}[\exp(-j\pi x/2)] - \tanh^{-1}[\exp(j\pi x/2)] \}. \quad (4d)$$

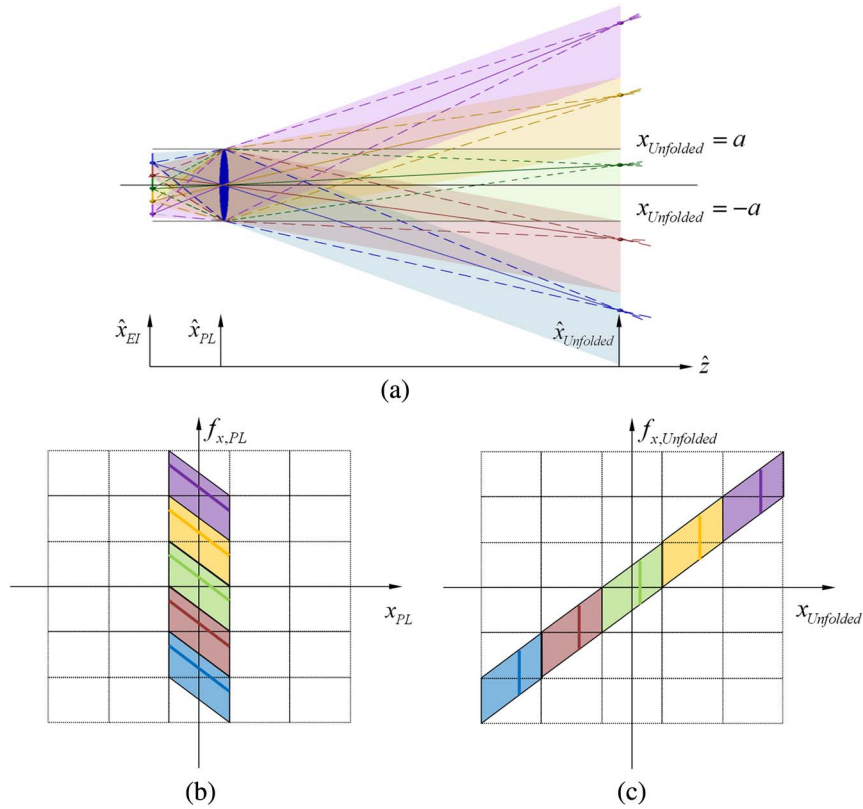


Fig. 4. (Color online) (a) Propagation of light field through the projection lens and WDFs at (b) projection lens plane and (c) image plane where there is no light tunnel and the dimension of a projected image is 5 times larger than that of the aperture stop of the projection lens.

In this folding effect, it is interesting that the sequence of views changes. This is clear by comparing the WDFs in Figs. 4(c) and 5(d). The stack of the partial WDFs in Fig. 5(d) does not just follow the

sequence of those in Fig. 4(c). This reason is understood by following the changes of the WDF according to the propagation of light field, as shown in Figs. 4(b) and 4(c). For example, the yellow part is

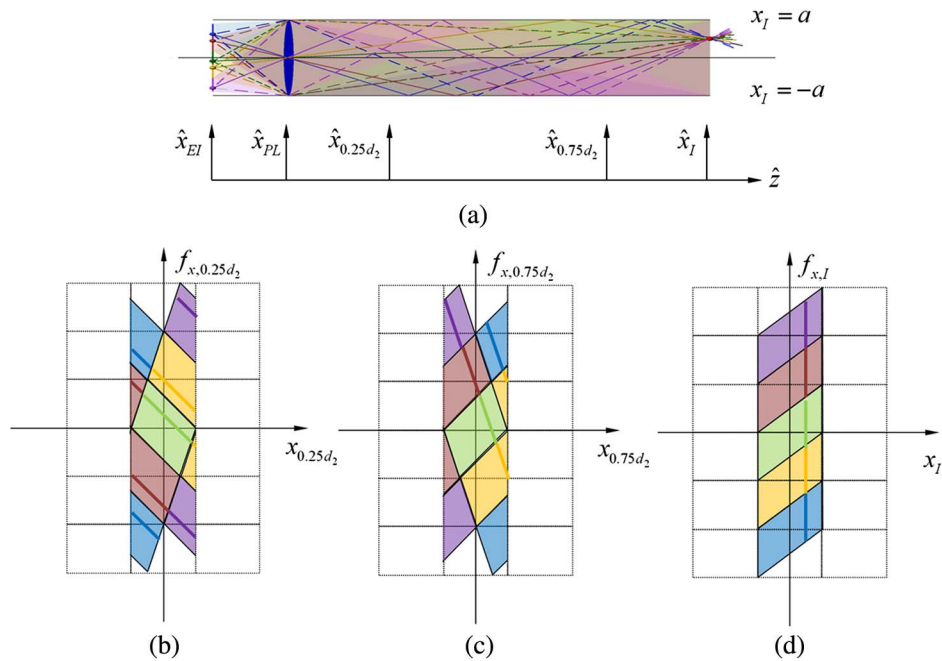


Fig. 5. (Color online) (a) Propagation of light field through the projection lens and the light tunnel and WDFs at (b) the plane with propagation distance as $0.25d_2$, (c) the plane with propagation distance as $0.75d_2$, and (d) the image plane when the light field is folded by the light tunnel and the dimension of a projected image is 5 times larger than that of the aperture stop of the projection lens.

next to the purple part before folding but these two parts are positioned apart from each other since the yellow part is folded only once even though the purple part is folded twice through the light tunnel. In addition, there is one thing more to notice. In Fig. 5(d), the shape of the WDF comprised of views is similar to that of general projection-type 3D displays such as integral imaging.

The viewing angle and the spatial resolution have a trade-off relation given by

$$N_{\text{Total}} = N_{\text{EI}} \times N_{\text{View}}. \quad (5)$$

Here, N_{EI} is the resolution of the elemental image and N_{View} is the number of the views displayed by this system. The product of these two parameters is equal to the total number of pixels comprising whole elemental images. The viewing angle is determined as

$$\Theta_{\text{EI}} = 2 \tan^{-1} \left(\frac{w}{2d_1} \right). \quad (6)$$

The width of the elemental image and the distances between the elemental image plane and the projection lens plane are involved to determine the focal length of the projection lens according to Eq. (2). So the viewing angle is also related by the focal length of the projection lens.

3. Generation of Elemental Images

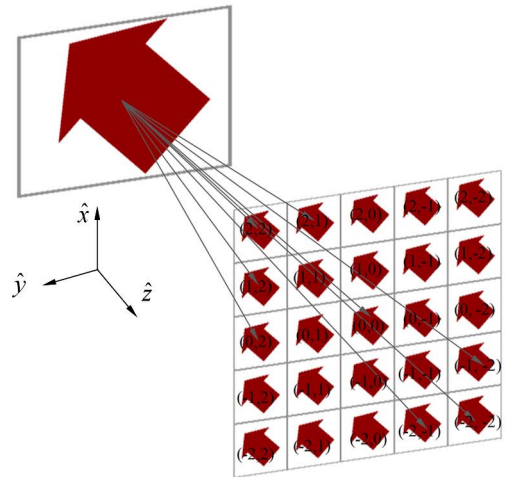
A 3D light-folded display with single projection lens presents full-parallax views since the light tunnel folds the light field both horizontally and vertically. The folding by mirrors changes the direction of view and flips the views spatially. Figure 6(a) shows the views conventionally defined by the positions where the observer watches the display. These are represented as an array of views and the subscripts are noted according to positions. The positions of each view are specified by the direction of chief rays passing through the center of the WDF. The central directional cosines of horizontally m th and vertically n th view are given by

$$\text{Directional cosine of View}_{mn} = \frac{mw}{d_1} \hat{f}_{xI} + \frac{nw}{d_1} \hat{f}_{yI}. \quad (7)$$

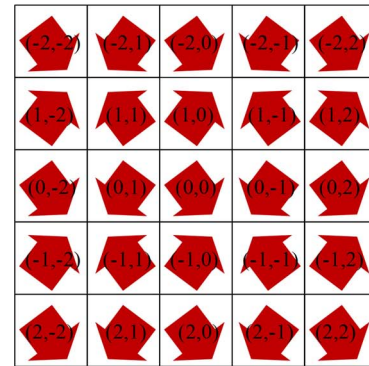
Here, each view is a function of (x_I, y_I) as

$$\text{View}_{mn} = \text{View}_{mn}(x_I, y_I). \quad (8)$$

The folding effect results in interesting relation between views and elemental images. Some elemental images are the same as the view but others are the flipped view horizontally, vertically, or both. In addition, the sequence of elemental images in the array needs to be different from that of views. Therefore,



(a)



(b)

Fig. 6. (Color online) (a) Views of objects depending on the viewing directions and (b) positions and rotations of individual views in array of elemental images.

the horizontally m th and vertically n th elemental image is related with the view as

$$\begin{aligned} \text{EI}_{mn}(x_{\text{EI}}, y_{\text{EI}}) \\ = \text{View}_{(-1)^{m+1}m(-1)^{n+1}n} \left[(-1)^{m+1} \frac{d_2}{d_1} x_I, (-1)^{n+1} \frac{d_2}{d_1} y_I \right]. \end{aligned} \quad (9)$$

From Eq. (9), the configuration of the array is shown in Fig. 6(b). The element in the center is represented as $\text{View}_{00}(-d_2/d_1 x_I, -d_2/d_1 y_I)$, where the signs in x_I and y_I are changed due to the projection lens. The ratio of the distances d_2/d_1 comes from the magnification. Orientations of the adjacent elemental images are determined as mirror symmetry to the central elemental image. The views of EI_{10} and EI_{00} meet each other by the bottom sides of them and the views of EI_{10} and EI_{01} meet each other by the left sides of them. This array of elemental images resembles the result obtained by punching with an arrow shape after folding of paper. Figure 7 shows an example of the array of elemental images, which is applied for the experiment in the next section.

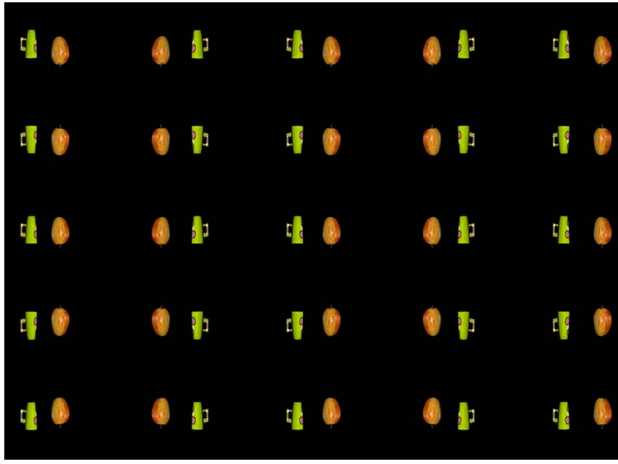


Fig. 7. (Color online) Array of elemental images applied for the experiment.

4. Experimental Results

The display is realized with small liquid crystal display (LCD) panels, a projection lens, and a light tunnel, as shown in Fig. 8. The elemental images are displayed on three LCD panels where each panel represents red, green, and blue color of images and whole images are combined by a beam combiner. Epson L3P07X is used as the LCD panel and it is a 0.7 in. diagonal panel and has 1024×768 resolutions. As a projection lens, Nikon AF-S Nikkor 35 mm 1:1.8 G is applied and from this choice the dimension of the light tunnel is determined. The aperture size of the light tunnel needs to be smaller than that of the projection lens. The length of the light tunnel is set as the magnification by the projection lens is equal to five and five-by-five different views are possible to be displayed in this setup.

The displayed images are taken by a camera with a telecentric lens. The telecentric lens provides the flexibility in measurement of an individual view. It

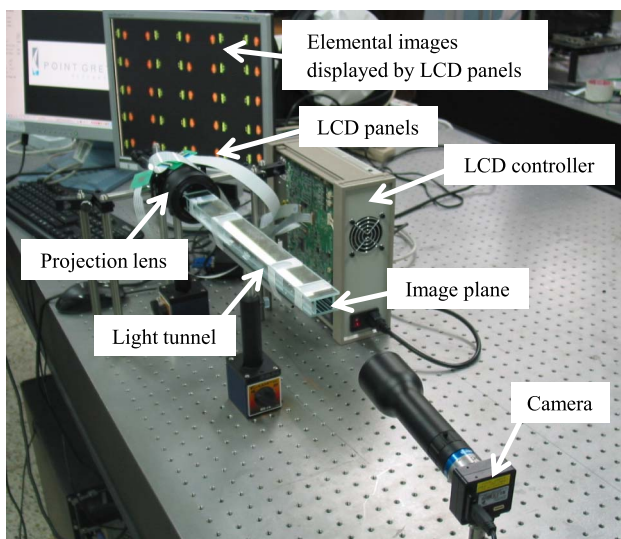


Fig. 8. (Color online) Experimental setup of the 3D light-folded display with one projection lens and the camera with telecentric lens for observation.

accepts only rays parallel to the optical axis and the capturing of views within reasonable distance is possible, which are similar to the images captured far from the display. As a telecentric lens, Edmund optics 0.30× Techspec is used and Pointgray CMLN-13S2C-CS is used for capturing images.

In this display, the view is defined as the image taken by the observer who stands infinitely far from the display. This situation is realized by using a telecentric lens. This image is different from the image taken by the observer who stands within a finite distance from the display. Usually when the distance from the observer to the display decreases, the number of the views increases, which the observer watches simultaneously. This image is a summation of the parts of the views. As previously discussed, the light field of the proposed system is similar to that of the projection-type 3D display. The images taken by the telecentric lens show the elemental image corresponding to individual view.

Figure 9 shows perspective views from the 3D light-folded display at different positions. Among 25 views, four views are shown. As mentioned in previous section, every view is numbered by the observation positions. Figures 9(a)–9(d) show View_{0,0}, View_{0,1}, View_{-2,0}, and View_{1,-2}, respectively. In every view, it is distinguishable that the relative positions of an apple and a cup change as designed.

Practically the light tunnel needs to be carefully manufactured. Figure 10 shows a simulation result when the multiple reflections happen with a wrongly manufactured light tunnel. In this case, right and upper sides of the light tunnel are assumed wrongly tilted. Under this assumption the elemental images are reversely calculated from the image plane with the same views to the elemental image plane. There are several ways elemental images can be seen by an observer. The elemental image, EI₁₁, has two chances to be displayed. One is reflected by the left side and

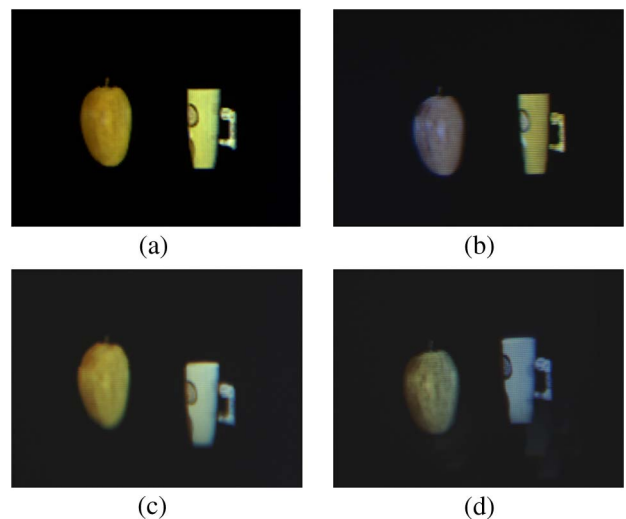


Fig. 9. (Color online) Perspective views of the 3D light-folded display with one projection lens at the positions; (a) View_{0,0}, (b) View_{0,1}, (c) View_{-2,0}, and (d) View_{1,-2}.

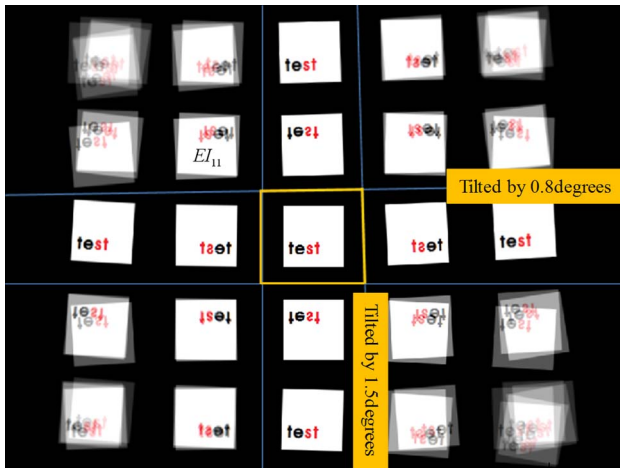


Fig. 10. (Color online) Reversely calculated array of elemental images under the condition mirrors in the light tunnel are wrongly tilted.

then reflected by the upper side of the light tunnel. The other is reflected by the upper side and then reflected by the left side. So if the mirrors of the light tunnel are not parallel to each other, the effect of this misalignment increases according as the number of reflection increases.

5. Conclusion

In general, projection-type 3D display is constructed with plural projection lenses since each different view is usually a projection of an elemental image that is assigned to the individual projection lens. In this paper, we propose an interesting way to realize a projection-type 3D display with single projection lens. A rectangular light tunnel placed right behind the projection lens folds the light field and finally several different views are imaged at the same position. By analyzing the WDF of this system, it is clear that it has the same light field as that of general integral imaging display. The system has a very simple structure and there is an advantage to reducing the number of projection lenses. We expect this approach is also applicable so that this system becomes made as a module easy to be stacked. Then the arrayed module may be a large 3D display that looks like a modified integral imaging with a light tunnel attached to each lens. This geometry may have a similar sensitive to the aberration of the projection lens in comparison of other projection-type 3D displays since the total field of view is not changed by using the light tunnel. This approach may make it easy to calibrate the system since the elemental images and the projection lens are modularized.

This research was partially supported both by Basic Science Research Program through the National Research Foundation of Korea (NRF) funded by the Ministry of Education, Science and Technology (2012R1A1A1014417) and by Kyungpook National University Research Fund, 2012.

References

1. J. Hong, Y. Kim, H.-J. Choi, J. Hahn, J.-H. Park, H. Kim, S.-W. Min, N. Chen, and B. Lee, "Three-dimensional display technologies of recent interest: principles, status, and issues," *Appl. Opt.* **50**, H87–H115 (2011).
2. B. Javidi and F. Okano, eds., *Three Dimensional Television, Video, and Display Technologies* (Springer, 2002).
3. Y. Takaki, "High-density directional display for generating natural three-dimensional images," *Proc. IEEE* **94**, 654–663 (2006).
4. A. Stern and B. Javidi, "3-D computational synthetic aperture integral imaging (COMPSAII)," *Opt. Express* **11**, 2446–2451 (2003).
5. H. Liao, M. Iwahara, H. Nobuhiko, and T. Dohi, "High-quality integral videography using a multiprojector," *Opt. Express* **12**, 1067–1076 (2004).
6. B. Lee, J.-H. Park, and S.-W. Min, "Three-dimensional display and information processing based on integral imaging," in *Digital Holography and Three-Dimensional Display*, T.-C. Poon, ed. (Springer, 2006), pp. 333–378.
7. G. E. Favalora, "Volumetric 3D displays and application infrastructure," *IEEE Comput.* **38**, 37–44 (2005).
8. A. Jones, I. McDowall, H. Yamada, M. Bolas, and P. Debevec, "Rendering for an interactive 360° light field display," *ACM Trans. Graph.* **26**, 40 (2007).
9. T. Georgiev, K. C. Zheng, B. Curless, D. Salesin, S. Nayar, and C. Intwala, "Spatio-angular resolution trade-offs in integral photography," in *Proceedings of the 17th Eurographics Workshop on Rendering* (Eurographics, 2006), pp. 263–272.
10. A. W. Lohmann, R. G. Dorsch, D. Mendlovic, Z. Zalevsky, and C. Ferreira, "Space-bandwidth product of optical signals and systems," *J. Opt. Soc. Am. A* **13**, 470–473 (1996).
11. M. A. Neifeld, "Information, resolution, and space-bandwidth product," *Opt. Lett.* **23**, 1477–1479 (1998).
12. M. J. Bastiaans, "Transport equations for the Wigner distribution function," *Opt. Acta* **26**, 1265–1272 (1979).
13. Z. Zhang and M. Levoy, "Wigner distributions and how they relate to the light field," in *Proceedings of IEEE International Conference on Computational Photography* (IEEE, 2009), pp. 1–10.
14. H. M. Ozaktas, M. A. Kutay, and Z. Zalevsky, *The Fractional Fourier Transform with Applications in Optics and Signal Processing* (Wiley, 2001).
15. T. Balogh, T. Forgács, T. Agocs, O. Balet, E. Bouvier, F. Bettio, E. Gobbetti, and G. Zanetti, "A scalable hardware and software system for the holographic display of interactive graphics applications," in *Eurographics Short Papers Proceedings* (Eurographics, 2005), pp. 109–112.
16. T. Agocs, T. Balogh, T. Forgacs, F. Bettio, E. Gobbetti, G. Zanetti, and E. Bouvier, "A large scale interactive holographic display," in *Proceedings of IEEE Conference on Virtual Reality* (IEEE, 2006), pp. 311–312.
17. J. Hahn, Y. Kim, and B. Lee, "Uniform angular resolution integral imaging display with boundary folding mirrors," *Appl. Opt.* **48**, 504–511 (2009).